

Antibacterial Application of Carpathian Clinoptilolite as Cetylpyridinium Carrier

Stepan Milyovich ¹, Valerii Pantyo ², Elvira Danko ³, Artem Pogodin ⁴, Mykhajlo Filep ^{4,5}, Oksana Fizer ^{6,*}, Maksym Fizer ⁶, Vasyl Sidey ⁷, Ruslan Mariychuk ⁸

¹ Department of Physical and Colloid Chemistry, Educational and Scientific Institute of Chemistry and Ecology, Uzhhorod National University, Fedinets' Str. 53/1, 88000, Uzhhorod, Ukraine; stepan.milyovich@uzhnu.edu.ua (S.M.);

² Department of Microbiology, Virology, and Epidemiology with the course of Infectious Diseases, Faculty of Medicine, Uzhhorod National University, Narodna Sq. 1, 88000, Uzhhorod, Ukraine; valerij.pantyo@uzhnu.edu.ua (V.P.);

³ Department of Dental therapy, Faculty of Dentistry, Uzhhorod National University, University Str. 16a, 88000, Uzhhorod, Ukraine; elvira.danko@uzhnu.edu.ua (E.D.);

⁴ Department of Inorganic Chemistry, Educational and Scientific Institute of Chemistry and Ecology, Uzhhorod National University, Fedinets' Str. 53/1, 88000, Uzhhorod, Ukraine; artempogodin88@gmail.com (A.P.);

⁵ Department of Biology and Chemistry, Ferenc Rákóczi II Transcarpathian Hungarian College of Higher Education, Kossuth Sq. 6, 90200, Beregovo, Ukraine; mfilep23@gmail.com (M.F.);

⁶ Department of Organic Chemistry, Educational and Scientific Institute of Chemistry and Ecology, Uzhhorod National University, Fedinets' Str. 53/1, 88000, Uzhhorod, Ukraine; oksana.fizer@uzhnu.edu.ua (O.F.), max.fizer@uzhnu.edu.ua (M.F.);

⁷ Research Institute for Physics and Chemistry of Solid State, Uzhhorod National University, Pidhima Str. 46, 88000, Uzhhorod, Ukraine; vasylysidey@yahoo.com (V.S.);

⁸ Department of Ecology, Faculty of Humanity and Natural Sciences, University of Presov, 17th November 1, 08116, Presov, Slovak republic; ruslan.mariychuk@unipo.sk (R.M.);

* Correspondence: oksana.fizer@uzhnu.edu.ua (O.F.);

Scopus Author ID 57200115316

Received: 22.06.2022; Accepted: 24.07.2022; Published: 30.07.2022

Abstract: A bactericidal and structural study on the "cetylpyridinium chloride-clinoptilolite" associates has been carried out. For the first time, the samples were synthesized using the powdered clinoptilolite from the Sokyrnytsia deposit (Transcarpathian region, Ukraine). Eight "cetylpyridinium chloride-clinoptilolite" associates have been synthesized using different cetylpyridinium chloride concentrations and further characterized by elemental analysis and FTIR techniques. The association of the cetylpyridinium cation with the zeolite anionic matrix has been studied. It was found that the adsorption of the cetylpyridinium cations occurs on the clinoptilolite surface without destroying the anionic zeolite framework. Furthermore, the antibacterial activity of the associates was analyzed, and a significant activity against *Staphylococcus aureus* and *Candida albicans* strains was observed, which is caused by the cetylpyridinium cation presence. Unmodified natural and acid-treated clinoptilolites did not show antibacterial activity; however, these can be effectively used as a matrix carrier for the cetylpyridinium cation.

Keywords: antimicrobial; bactericide; cetylpyridinium; clinoptilolite; DTA; FTIR; zeolite.

© 2022 by the authors. This article is an open-access article distributed under the terms and conditions of the Creative Commons Attribution (CC BY) license (<https://creativecommons.org/licenses/by/4.0/>).

1. Introduction

The development of new antibacterial [1,2], antifungal [3], and antiviral [4] drugs is still an actual task of modern medicine, pharmacology, and chemistry. One of the powerful methods for developing new medicines is the modification of well-known drugs. In a few of our previous papers, we have investigated some cetylpyridinium-based compounds, which

potentially have various applications as ionophores [5], ionic liquids [6], or antibacterials [7]. Moreover, cetylpyridinium chloride (CPC) can be used as a titrant in the potentiometric determination of anionic analytical forms of different lipophilicity [8-11]. To extend the list of potential applications of cetylpyridinium (CP) derivatives, we have decided to develop a CP-containing compound with antibacterial action on pathogenic bacteria stamps. The actuality of the development of CP-containing compositions is confirmed by the numerous recent papers devoted to the antibacterial action of cetylpyridinium chloride [12-16]. A zeolite has been selected as a modifier. This selection was dictated by various properties and applications characteristic of cetylpyridinium-zeolite compounds. For example, Li et al. have utilized cetylpyridinium bromide-treated clinoptilolite as an effective absorber for the ammonium, nitrate, and phosphate ions [17]. Similarly, Prajitno et al. have used natural clinoptilolite modified with the cetylpyridinium cation for the flotation of cesium [18]. Cetylpyridinium-modified zeolites can also be used for the absorbance of heavy metals [19], dyes [20], polycyclic aromatic hydrocarbons [21], and toxins [22]. Moreover, it was shown that zeolites immobilized with the CP cation could be utilized as antibacterials in dentistry [23,24].

Since the spread of the COVID-19 pandemic, antiseptic prices have risen considerably. Therefore, developing new effective biocide substances based on low-cost components (CPC and clinoptilolite) remains relevant. We obtained and examined a series of CPC-clinoptilolite samples in the present study by treating powdered clinoptilolite from the Sokyrnytsia deposit (Transcarpathian region, Ukraine) with CPC water solutions. It should be highlighted that the content of clinoptilolite in the zeolite tuff of this deposit reaches 85%, which is a high value compared with other deposits, and this allows excluding an enrichment stage of the material's raw. The non-zeolite component of the tuff does not contain harmful substances (like asbestos), often found in zeolite tuffs. Moreover, as the tuff extraction at the Sokyrnytsa deposit is carried out in an open-pit way, and since the deposit itself is located at the center of Europe, the price of the raw material for the European market is reasonably low.

2. Materials and Methods

2.1. Chemicals.

CPC monohydrate (reagent grade) and hydrochloric acid solution (chemically pure grade) were purchased from "Sfera Sim" company (Lviv, Ukraine). Silver nitrate (analytical reagent grade) was purchased from Merck. Double distilled water was used in all experiments.

2.2. Equipment.

Fourier-transform infrared spectra (FTIR) were recorded on a Shimadzu IRPrestige-21 spectrometer in attenuated total reflection (ATR) mode using MIRacle ATR accessory (PIKE) with a zinc selenide crystal. Computations were performed on a workstation containing 256 GB of RAM and twenty processor cores. Elementar Vario MICROcube was used for the measurement of elemental composition. Differential thermal analysis (DTA) was carried out according to the standard technique [25] in the static air atmosphere using a combined K-type thermocouple (accuracy of ± 5 °C) as a temperature sensor. High-purity pre-calcined Al₂O₃ (99.9999% purity) was used as reference material. Measurements were performed using an open quartz sample vessel in the temperature range of 20-870 °C and the scan heating rate at 700 °C/h. Determination of the temperature of the effects on DTA curves was carried out as proposed in [26]. Powder patterns of investigated zeolite samples were recorded using an

AXRD Benchtop diffractometer (Proto Manufacturing Limited, USA) in the Bragg-Brentano $\theta/2\theta$ shooting geometry with the Ni-filtered $\text{CuK}\alpha$ radiation and exposition of 1 s. The polycrystalline samples were ground in an agate mortar and sifted through the same sieves to avoid unwanted lines expansion through different particle sizes.

2.3. Samples preparation.

The clinoptilolite rock of the Sokyrnytsia deposit, which has a green-blue color with a clinoptilolite content in the tuff of about 80%, was used for the present work. To obtain the starting material, a clinoptilolite tuff was ground, and certain fractions of grain size less than 14 μm were selected, washed with distilled water, and then dried. In this way, the CL-0 form was obtained. The hydrogen form of clinoptilolite (CL-H) was synthesized by treating the CL-0 form with a 1 mol/L solution of hydrochloric acid for 8 hours in a water bath at 90 °C. After modification, the samples were thoroughly washed with distilled water until a negative test for chloride ions was reached and then dried in air. The absence of chloride anions was monitored with a 1% aqueous solution of silver nitrate.

To prepare the CPC-modified clinoptilolite samples, 5.0 g of the clinoptilolite CL-0 or CL-H were mixed with the 200 mL of CPC solution (1.0 mmol/L, or 5.0 mmol/L, or 10.0 mmol/L). The resulting suspension was stirred overnight, and the final precipitate was filtered with a water pump on a Buchner funnel. The filter residue was washed with two 20 mL portions of double distilled water to separate weakly bound CPC molecules. The obtained CPC-modified clinoptilolites and their code names are presented in Table 1.

Table 1. CPC-modified clinoptilolite samples: preparation and code names.

Sample	Preparation
CL-0	powder of natural clinoptilolite with a size diameter < 100 μm
CL-0-CPC-1	CL-0 treated with 1.0 mmol/L CPC solution
CL-0-CPC-5	CL-0 treated with 5.0 mmol/L CPC solution
CL-0-CPC-10	CL-0 treated with 10.0 mmol/L CPC solution
CL-H	CL-0 treated with 1 mol/L HCl at 90 °C for 8 hours
CL-H CPC-1	CL-H treated with 1.0 mmol/L CPC solution
CL-H CPC-5	CL-H treated with 5.0 mmol/L CPC solution
CL-H CPC-10	CL-H treated with 10.0 mmol/L CPC solution

2.4. Antibacterial activity preparation.

The antimicrobial activity of the CL-0-CPC-10 and CL-H-CPC-10 samples was determined against clinical isolates of *S. aureus*, *C. albicans*, *E. coli*, *K. pneumonia*, and *P. aeruginosa*. Specified microorganisms were isolated from the patients with chronic generalized periodontitis and identified using bacterioscopical, bacteriological, and biochemical methods. Since the CL-0-CPC-10 and CL-H-CPC-10 substances are insoluble in water, the study was performed according to the following scheme: in Eppendorf tubes with a volume of 2 mL, different portions of test substances (100, 50, 25, and 10 mg) were made. Next, a standardized inoculum of microorganisms was prepared (daily agar cultures, adjusted to a turbidity standard of 0.5 according to McFarland and diluted 100-fold), which was added in a volume of 0.5 mL to each tube.

Next, the contents of the tubes were thoroughly mixed and incubated in a thermostat at 37 °C for 24 hours. The growth of microorganisms in test tubes was determined by reseeded their contents (0.05 mL) on solid nutrient media in Petri dishes with nutrient agar. The growth intensity on Petri dishes was measured in four degrees: "I" – the absence of growth; "II" – poor growth (1-30 colonies); "III" – abundant growth (many distinguished colonies); "IV" –

continuous growth of microorganisms. Control tubes contained 0.5 mL of microbial inoculum without test substances. Additionally, the antimicrobial activity of zeolites CL-0 and CL-H in the amount of 100 mg was studied.

3. Results and Discussion

3.1. Composition and structure of CPC-clinoptilolite samples.

The elemental analysis of the synthesized CPC-clinoptilolite samples was performed in triplicate by using an Elementar Vario MICROcube automatic CHNS-analyzer. The obtained average values are summarized in Table 2. As can be seen, none of the samples contains the sulfur element, which is some kind expected. Analogously, no nitrogen was identified in the samples, which is unexpected at first glance. However, we should mention that the calculated nitrogen content in a CP cation is only 4.60%. The nitrogen content became indeterminate in the case of low CP-content association with the clinoptilolite. The hydrogen content is not too informative, as this parameter is sensitive to the storing conditions, primarily moisture and temperature.

On the other hand, the carbon content is the most reliable parameter for estimating the composition of the formed CPC-clinoptilolite samples. Using a more concentrated CPC solution leads to an increased carbon content (and, therefore, a CP cation content) in the target samples, which is reasonably expected. And which was less expected is the less carbon content, and thus CP cations, in the case of acidic forms of the clinoptilolite CL-H. At first, it was suggested that the ionic exchange would be preferable in the case of acidic form. However, the anionic matrix of clinoptilolite contains the tetrahedral aluminate AlO_4^- fragments that determine the cation-exchange properties of zeolites. These aluminate fragments are acid-sensitive and can be destroyed by the action of acid, which decreases the ability of zeolite to associate with cations. This assumption was confirmed by the Si/Al-elemental analysis made in the previous work [27], where authors have shown that the treatment of zeolite with hydrochloric acid leads to a decrease in aluminum content and thus the number of anionic centers, which can take place in ion exchange decreases also.

Table 2. Elemental analysis of CPC-clinoptilolite samples.

	C, %	H, %
CL-0	0.00	1.85
CL-0-CPC-1	0.99	0.79
CL-0-CPC-5	1.72	1.04
CL-0-CPC-10	1.87	0.92
CL-H	0.00	0.58
CL-H-CPC-1	0.80	0.78
CL-H-CPC-5	1.07	0.81
CL-H-CPC-10	1.14	0.88

Normalized FTIR spectra of the CL-0 series are presented in Figure 1. There is no considerable difference between the spectra, except in the region of $2800\text{--}3000\text{ cm}^{-1}$, where the C–H vibrations are observed. The peaks at 780 and 800 cm^{-1} correspond to the Al/Si–O symmetric stretching; a wide and very intense region of $917\text{--}1210\text{ cm}^{-1}$ with a maximum at 1032 cm^{-1} corresponds to the asymmetric Al/Si–O stretching. A wide signal at 1632 cm^{-1} is caused by the chemically bounded water molecules' H–O–H bending. A wide depth at 3615 cm^{-1} is due to water molecules' symmetric and asymmetric O–H stretching.

The peaks at 2848 cm^{-1} and 2916 cm^{-1} correspond to the symmetric and asymmetric C–H stretching vibrations of the cetyl chain of the CP cation. It is clear that the peak intensity of C–H vibrations increases with an increase in the CPC solutions' concentration.

FTIR spectra of the CL-H samples are shown in Figure 1 (b-e). Similarly to the CL-0 series, the vibrations related to the Al/Si–O and O–H stretching are clearly observed in the CL-H samples. The cetyl chain C–H stretching vibrations are observed as two peaks at 2856 cm^{-1} and 2924 cm^{-1} . Analogously to the CL-0 series, there can be tracked that the peak intensity depends upon the concentration of a CPC solution used for the treatment of starting clinoptilolite.

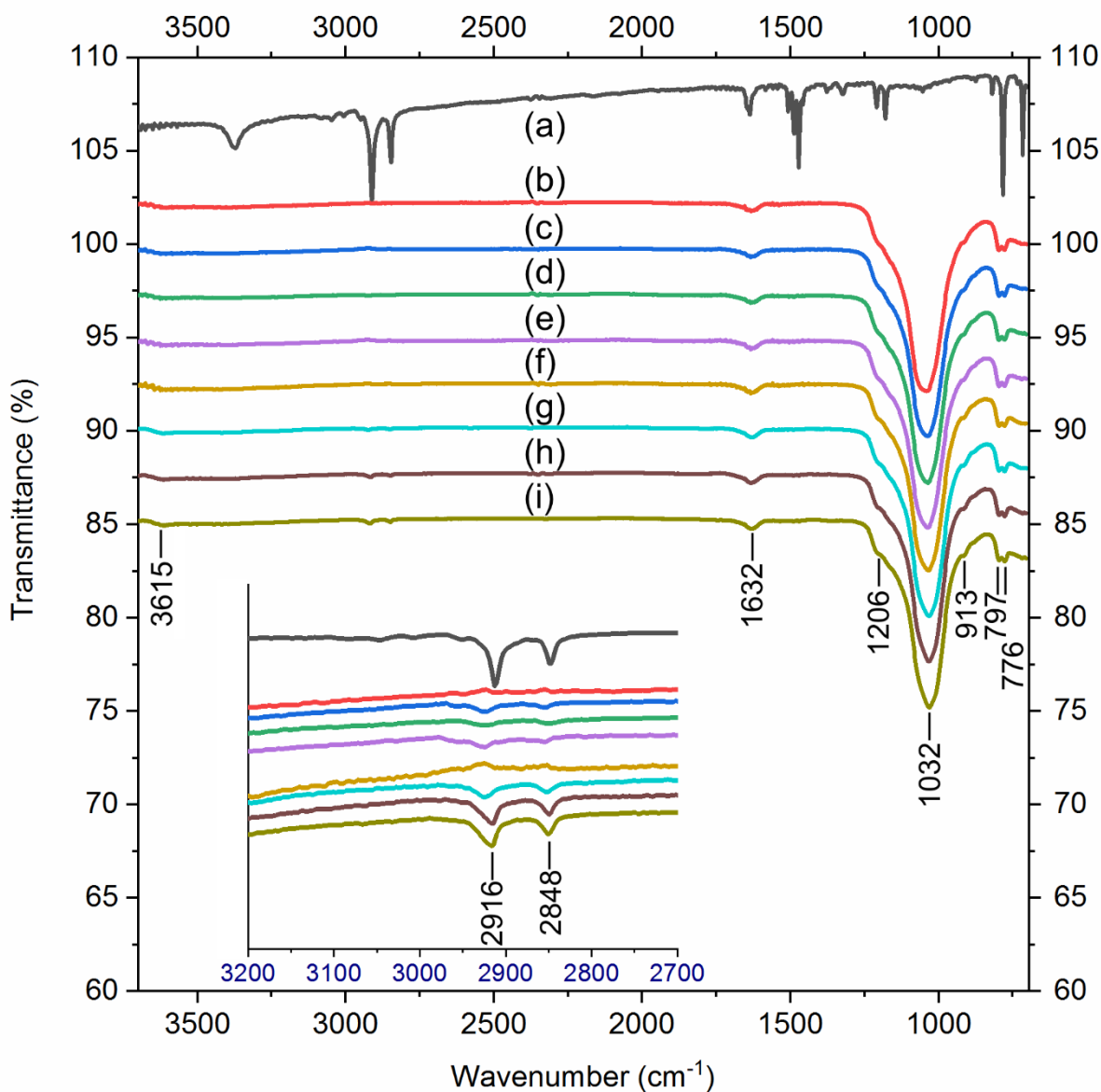


Figure 1. (a) FTIR spectra of CPC monohydrate and normalized FTIR spectra of (b) CL-H, (c) CL-H-CPC-1, (d) CL-H-CPC-5, (e) CL-H-CPC-10, (f) CL-0, (g) CL-0-CPC-1, (h) CL-0-CPC-5, and (i) CL-0-CPC-10. A region of $2600\text{--}3200\text{ cm}^{-1}$ is zoomed in on the inset.

To better understand the interaction of clinoptilolite with the CP cation, the analysis of the size of pores in the clinoptilolite structure and the size of the CP cation should be analyzed. Figures 2a-b show the sizes of the most important channels in the clinoptilolite structure. Moreover, the dimensions of the CP cation obtained from the X-ray single-crystal structure were considered [28] (Figure 2c). At first glance, it can be supposed that the CP cation can fit

into the clinoptilolite structure via the relatively large 12-ring pores. However, the effective pore size of the zeolite excludes molecules larger than $\sim 4 \text{ \AA}$ [29]. This can be explained by the non-zero van der Waals radius of atoms, which significantly reduces the effective interatomic distances and, thus, the pore size. At the same time, the size of the pyridinium "hydrophilic head" in the CP cation should be increased by at least the radius of hydrogen atoms, which can be taken as $1.09\text{--}1.20 \text{ \AA}$ [30]. In such a case, the radius of the CP head can be considered as about 8 \AA , which is twice the size of the effective pore size. Considering all the above, we have concluded that the CP cations should be associated with the clinoptilolite on its surface rather than be embedded in its anionic matrix. This allows us to suggest that the CPC-clinoptilolite compounds can be suitable transporting/conservation forms of the CP cation. Considering the well-known antibacterial activity of the cetylpyridinium compounds, in the next stage of our study, it was decided to analyze the activity of the synthesized CPC-clinoptilolite samples against various pathogenic microorganisms.

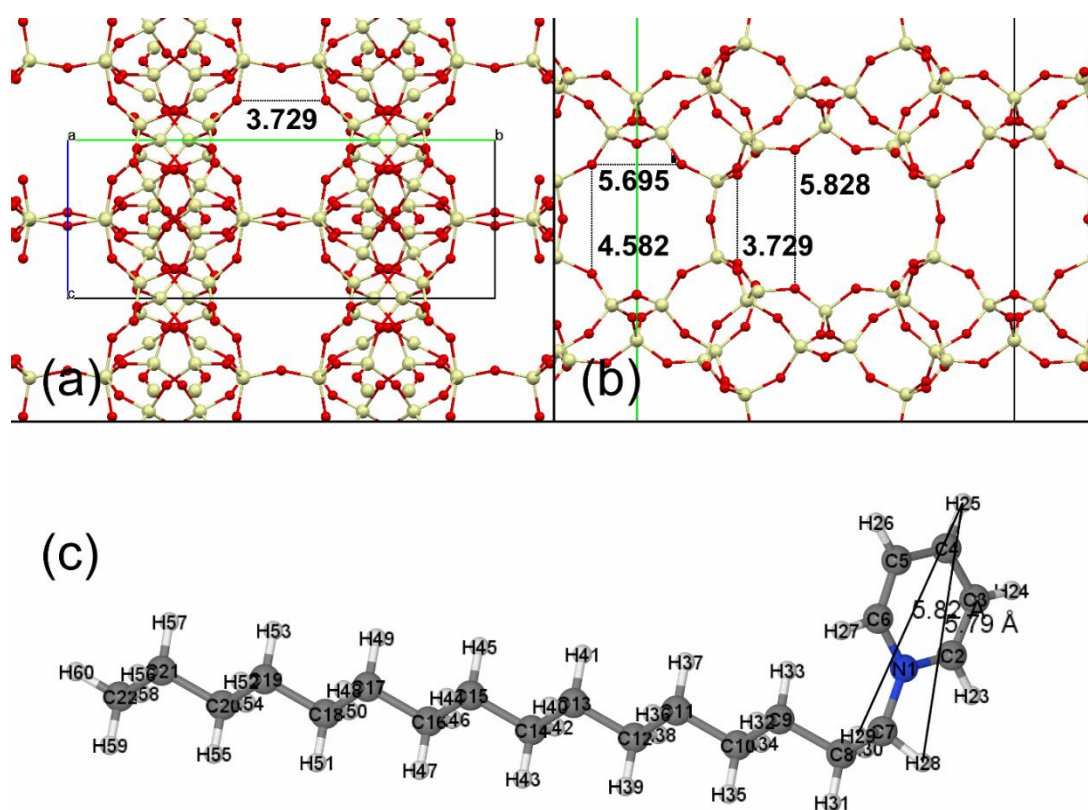


Figure 2. (a) General view of the clinoptilolite lattice from the *a* side; (b) general view of the clinoptilolite lattice from the *c* side; (c) general view of the cetylpyridinium cation. The interatomic distances are given in Å.

The curves of the differential thermal analysis (DTA) of the CL-0 and CL-0-CPC-10 samples are present in Figure 3. The DTA results have shown that the most considerable effects are related to the elimination of the water molecules, which can be divided into three different types. Physically bound water is removed first, corresponding to the endothermic effect at $73 \text{ }^\circ\text{C}$. Water molecules bounded to the non-frame cations and aluminum can be removed in the temperature range of $100\text{--}400 \text{ }^\circ\text{C}$. The water molecules of silanol surface groups "hydroxyl water" are removed at about $540 \text{ }^\circ\text{C}$. The lack of a clear CPC melting endothermic effect can be explained by its overlay with the water extraction effects. The notable endothermic effect at $354 \text{ }^\circ\text{C}$ in the case of the CL-0-CPC-10 sample corresponds to the CPC decomposition, whereas the exothermic effect at $799 \text{ }^\circ\text{C}$ should be attributed to the combustion of the CPC

decomposition products. It should also be highlighted that after the DTA experiment, the mass of the CL-0 and CL-0-CPC-10 samples have been reduced by 11.6% and 13.4%, respectively. This fact additionally testifies to the adsorption of CPC onto zeolite. The difference between the mass losses equals 1.8%, which perfectly matches the elemental analysis data.

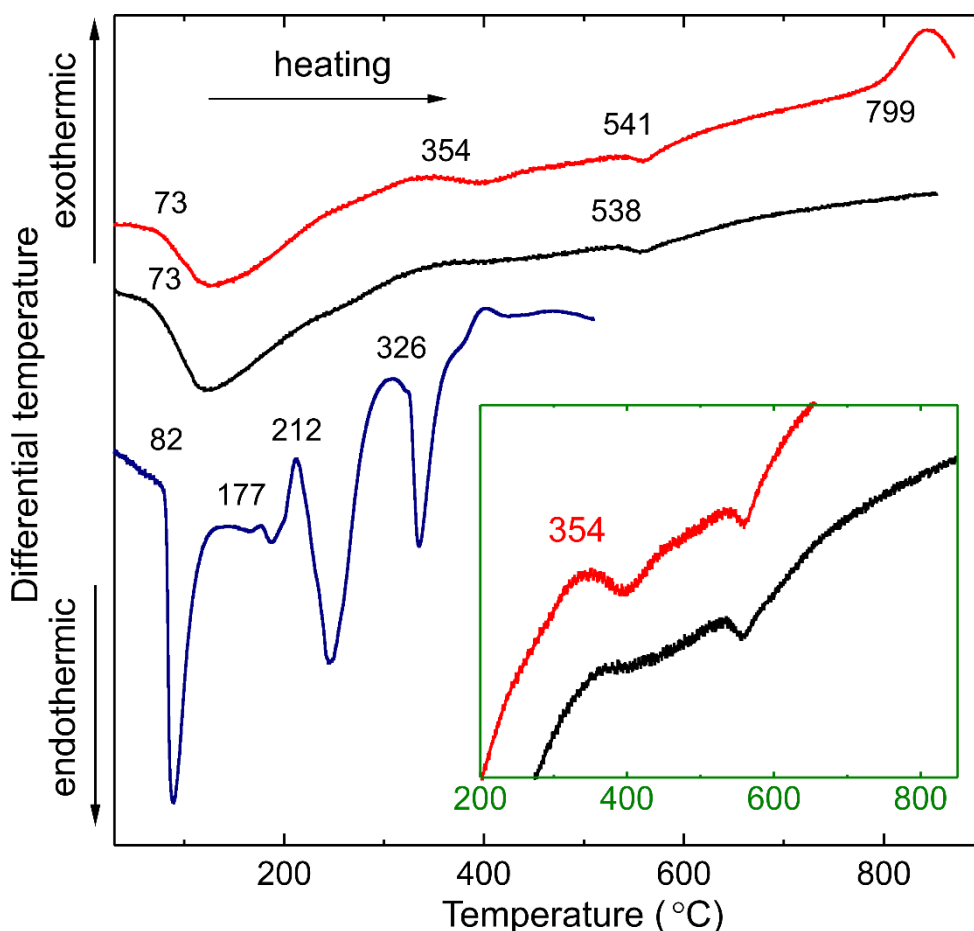


Figure 3. DTA curves of CPC monohydrate (blue line), CL-0 (black line), and CL-0-CPC-10 (red line).

Experimental powder patterns are shown in Figure 4. The phase analysis was performed by comparison of the experimental and available in the diffractometer's database cards. The phase content of the investigated samples corresponds to the mineral clinoptilolite. The diffraction patterns of the initial zeolite (CL-0) and modified ones (CL-0-CPC-10, CL-H, CL-H-CPC-10) are similar. This indicates that chemical treatment of natural clinoptilolite does not lead to changes in the crystal structure. Also, it is observed that the acid treatment of zeolite (CL-H, CL-H-CPC-10) leads to a slight increase in intensity due to the dissolution of fine fractions from pores. The peak intensity of CL-H-CPC-10 is less than for CL-H, which can be explained by the adsorption of CP on the surface of clinoptilolite.

The absence of the characteristic intensive peaks of CPC (Figure 4e) at $\sim 6^\circ$, $\sim 16^\circ$, and $\sim 19^\circ$ in the powder patterns of CL-0-CPC-10 and CL-H-CPC-10 testifies the absence of the CPC crystalline phase in these samples. In combination with the FTIR analysis, it justifies the idea of the adsorption of the cetylpyridinium cations on the surface of clinoptilolite rather than the formation of a mechanical mixture of clinoptilolite and CPC.

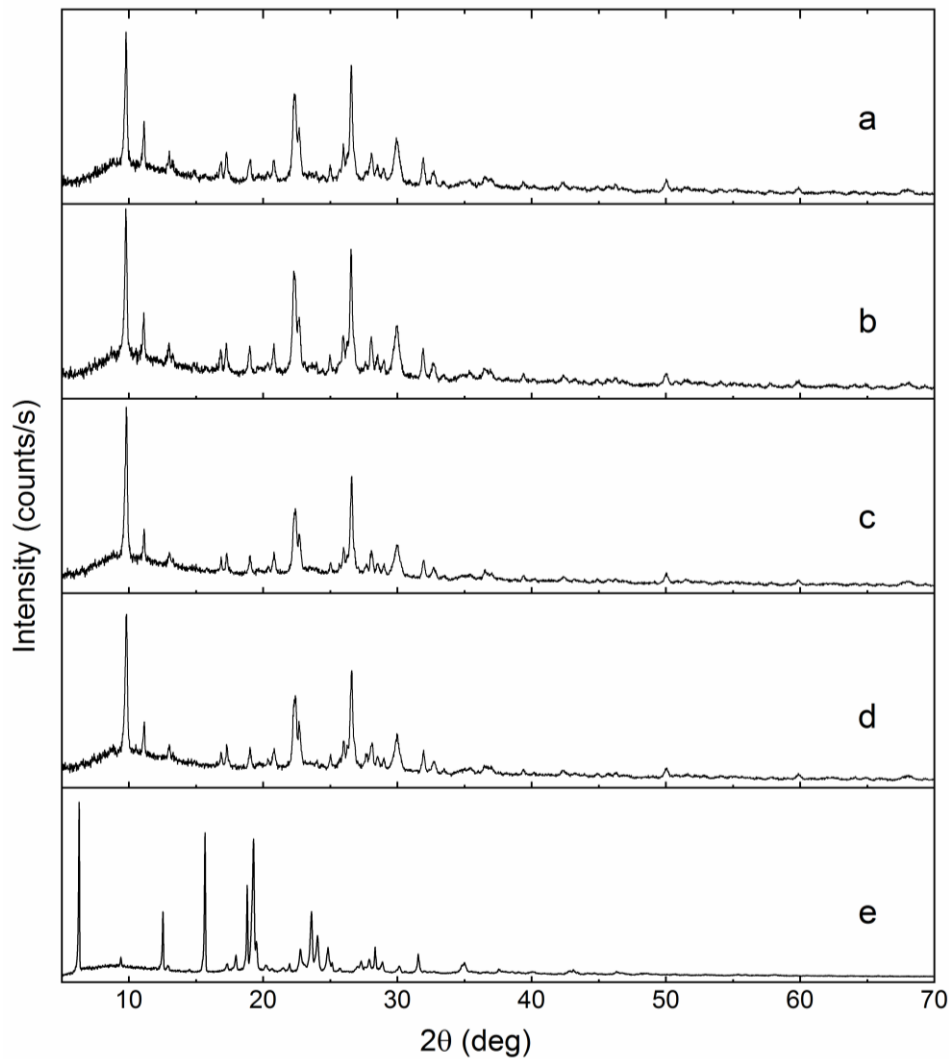


Figure 4. Powder patterns of investigated zeolite samples: CL-0 (a), CL-0-CPC-10 (b), CL-H (c), CL-H-CPC-10 (d), CPC monohydrate (e).

3.2. Antibacterial activity of CPC-clinoptilolite samples.

Figure 5 shows the plot of the antibacterial action of CPC-clinoptilolites against five microorganisms strains (*C. albicans*, *S. aureus*, *E. coli*, *K. pneumonia*, and *P. aeruginosa*) after cultivation with different quantities of the CL-0/H-CPC-10 substance, as well as with the CL-0 and CL-H clinoptilolites and without any additives (control). The percentage of growth was calculated as the ratio between the area of bacteria growth and the initial agar medium seeded area multiplied by one hundred. As the *E. coli*, *K. pneumonia*, and *P. aeruginosa* bacteria were less sensitive to the CPC-clinoptilolites, the experiments with pure zeolites were omitted for these microorganisms. An example of Petri dishes after reseeding *C. albicans* and *S. aureus* is presented in Figure 6.

It was found that the studied substances showed pronounced antimicrobial activity against some microorganisms. Thus, 10 mg of CL-0-CPC-10 only slightly inhibited the growth rate of the studied strain of *C. albicans*, manifested by a decrease in growth rate compared with the control. Pure clinoptilolite CL-0 doesn't show antimicrobial activity – the growth identical to control was observed. In turn, the CL-0-CPC-10 substances in the amount of 25, 50, and 100 mg almost completely inhibited the growth of yeast-like fungi *C. albicans* (also see Figure 6a).

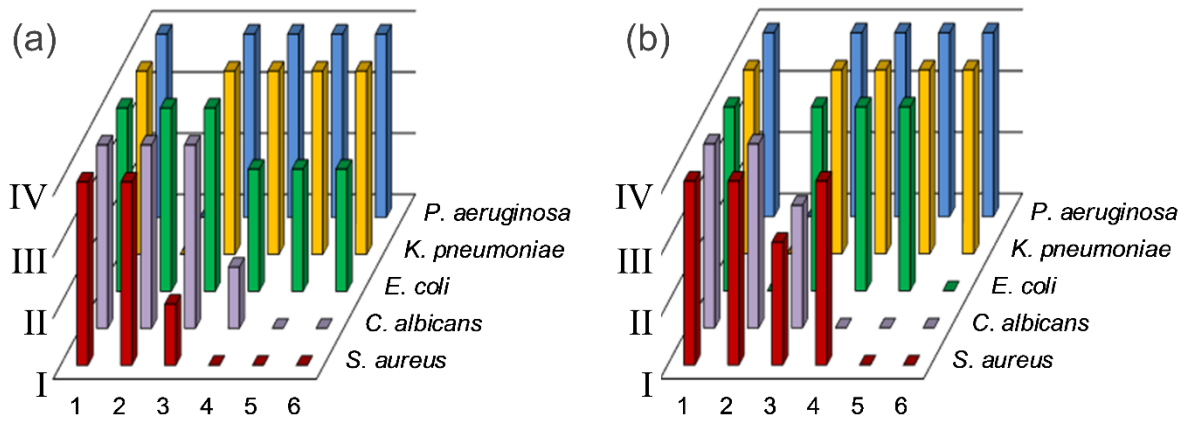


Figure 5. Antibacterial action of CPC-clinoptilolites. Percentage of growth area after reseeding: 1 – control, 2 – 100 mg of pure CL-X zeolite, 3 – 10 mg of CL-X-CPC-10, 4 – 25 mg of CL-X-CPC-10, 5 – 50 mg of CL-X-CPC-10, 6 – 100 mg CL-X-CPC-10, where, X can be 0 (a) or H (b). I – the absence of growth; II – poor growth (1-30 colonies); III – abundant growth (many distinguished colonies); IV – continuous growth of microorganisms.

From Figure 5b, it is clear that the pure CL-H zeolite, as well as 10 mg of CL-H-CPC-10, inhibit the growth of *C. albicans* only partially, while the increase of the amount of CL-H-CPC-10 to 25 mg or more leads to the complete inhibition of the growth of the studied strain of *C. albicans*. Figure 6b shows the growth of *C. albicans* after cultivation with the CL-H-CPC-10 sample.

Significant inhibition of *S. aureus* growth should be noted when cultivated with the CL-0-CPC-10 substance already in the amount of 10 mg (Figure 5a). When cultured in test tubes with the CL-0-CPC-10 quantities of 25-100 mg, the growth of the studied strain of *S. aureus* was completely inhibited. When cultivated with the pure zeolite CL-0, the growth rate of *S. aureus* was similar to the control (Figure 6c).

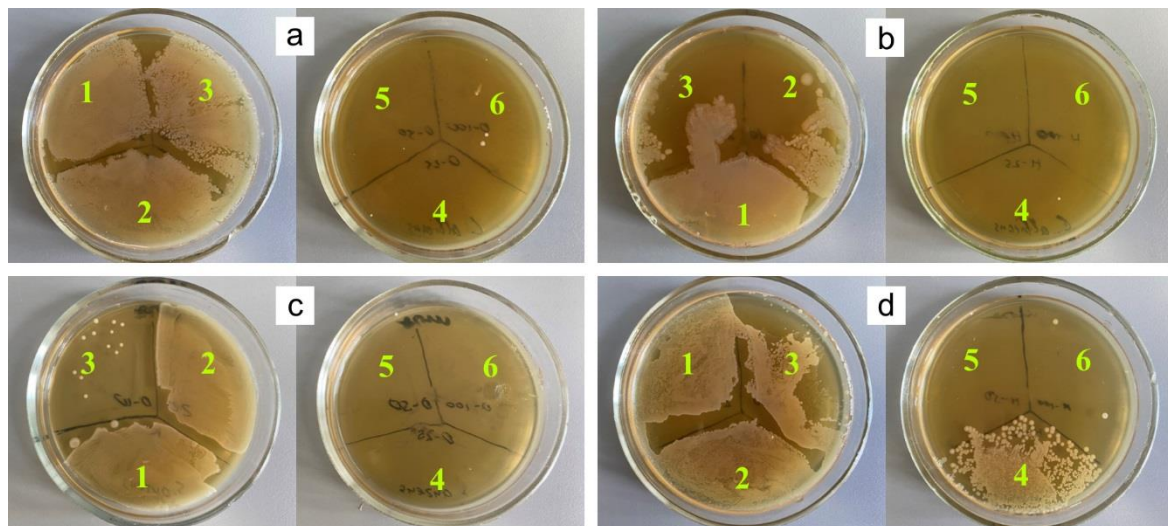


Figure 6. Antibacterial action of CPC-clinoptilolites. Growth of *C. albicans* (a, b) and *S. aureus* (c, d) on Petri dishes after reseeding: 1 – control, 2 – 100 mg of pure CL-X zeolite, 3 – 10 mg of CL-X-CPC-10, 4 – 25 mg of CL-X-CPC-10, 5 – 50 mg of CL-X-CPC-10, 6 – 100 mg CL-X-CPC-10, where, X can be 0 (a,c) or H (b,d).

From Figure 5, the CL-H-CPC-10 substance is less active against *S. aureus* as compared to the CL-0-CPC-10 substance. Thus, only after the cultivation with CL-H-CPC-10 in quantities of 50 and 100 mg was the growth of *S. aureus* completely inhibited, while in the case of 10 and 25 mg of CL-H-CPC-10, the growth was only partially inhibited. The acidic

form of clinoptilolite CL-H did not show antimicrobial activity against *S. aureus*. Figures 6d show the growth of *S. aureus* after cultivation with different amounts of the CL-H-CPC-10 sample.

Identical studies were performed on bacteria *E. coli*, *K. pneumonia*, and *P. aeruginosa*. In the case of *E. coli*, it should be noted that at different quantities of CL-0-CPC-10, the growth of *E. coli* is not inhibited completely but only partially suppressed. However, the CL-H-CPC-10 sample in the amount of 100 mg showed an antimicrobial effect on the studied *E. coli* strain. In the case of *K. pneumonia* and *P. aeruginosa* bacteria, the lack of antimicrobial effect was noted even when using CL-0-CPC-10 or CL-H-CPC-10 at an amount of 100 mg. Also, clinoptilolites CL-0 and CL-H were not studied as antimicrobials against *E. coli*, *K. pneumonia*, and *P. aeruginosa*, as these were not active against first studied *C. albicans* and *S. aureus*.

The presence of the cetylpyridinium cations has determined the antibacterial activity of the synthesized composites. The preferential antibacterial activity of the prepared composites matches other studies' results, where pure, unmodified CPC was explored [31-33].

4. Conclusions

The treatment of powdered clinoptilolite from the Sokyrnytsia deposit (Transcarpathian region, Ukraine) with aqueous solutions of cetylpyridinium chloride leads to the adsorption of the cetylpyridinium cation on the surface of the clinoptilolite samples. This was confirmed by the elemental analysis, FTIR spectra analysis, and DTA. No structural changes in the clinoptilolite framework were observed by means of the XRD analysis.

According to the microbiological studies, it can be stated that the CL-0-CPC-10 and CL-H-CPC-10 substances showed a pronounced antimicrobial effect against the studied isolates of *Staphylococcus aureus* and *Candida albicans*. However, only at a high amount (about 100 mg) the samples CL-0-CPC-10 and CL-H-CPC-10 showed a medium and high antibacterial effect against *Escherichia coli*; no antimicrobial activity was detected against the studied strains of *K. pneumonia* and *P. aeruginosa*. It was determined that acid treatment of clinoptilolite has almost no effect on the antibacterial activity of clinoptilolite-cetylpyridinium associates. In all cases, the antibacterial action is conditioned by the presence of the cetylpyridinium cation in the "clinoptilolite-cetylpyridinium" associates. Although the untreated zeolite and its acid form do not show an antibacterial effect, they can effectively act as a matrix for CP, which was demonstrated by our results.

Funding

This study was partially supported by the Ministry of Education and Science of Ukraine (0120U100431) and by the Slovak Academic Information Agency (National Scholarship Programme of the Slovak Republic, Grants ID 32706 and ID 35558).

Conflicts of Interest

The authors declare no conflict of interest.

References

1. Cui, X.; Lü, Yu.; Yue, C. Development and research progress of anti-drug resistant bacteria drugs, *Infect. Drug. Resist.* **2021**, *14*, 5575-5593. <https://doi.org/10.2147/IDR.S338987>.

2. Boyd, N.K.; Teng, C.; Frei, C.R. Brief overview of approaches and challenges in new antibiotic development: a focus on drug repurposing. *Front. Cell. Infect. Microbiol.* **2021**, *11*, 68451517. <https://doi.org/10.3389/fcimb.2021.684515>.
3. Bouz, G.; Doležal, M. Advances in antifungal drug development: an up-to-date mini review. *Pharmaceuticals* **2021**, *14*, 1312. <https://doi.org/10.3390/ph14121312>.
4. Adamson, C.S.; Chibale, K.; Goss, R.J.M.; Jaspars, M.; Newman, D.J.; Dorrington, R.A. Antiviral drug discovery: preparing for the next pandemic. *Chem. Soc. Rev.* **2021**, *50*, 3647-3655. <https://doi.org/10.1039/D0CS01118E>.
5. Fizer, M.; Fizer, O.; Sidey, V.; Mariychuk, R.; Studenyak, Ya. Experimental and theoretical study on cetylpyridinium dipicrylamide – a promising ion-exchanger for cetylpyridinium selective electrodes. *J. Mol. Struct.* **2019**, *1187*, 77-85. <https://doi.org/10.1016/j.molstruc.2019.03.067>.
6. Fizer, M.; Filep, M.; Fizer, O.; Fricova, O.; Mariychuk, R. Cetylpyridinium picrate: spectroscopy, conductivity and DFT investigation of the structure of a new ionic liquid. *J. Mol. Struct.* **2021**, *1229*, 129803. <https://doi.org/10.1016/j.molstruc.2020.129803>.
7. Fizer, O.; Filep, M.; Pantyo, V.; Danko, E.; Fizer, M. Structural study and antibacterial activity of cetylpyridinium dodecyl sulfate ion pair. *Biointerface Res. Appl. Chem.* **2022**, *12*, 3501-3512. <https://doi.org/10.33263/BRIAC123.35013512>.
8. Sakač, N.; Madunić-Čačić, D.; Marković, D.; Hok, L.; Vianello, R.; Šarkanj, B.; Đurin, B.; Hajdek, K.; Smoljan, B.; Milardović, S.; Matasović, B.; Jozanović, M. Potentiometric surfactant sensor based on 1,3-dihexadecyl-1*H*-benzo[d]imidazol-3-ium for anionic surfactants in detergents and household care products. *Molecules* **2021**, *26*, 3627. <https://doi.org/10.3390/molecules26123627>.
9. Fizer, O.; Fizer, M.; Sidey, V.; Studenyak, V. Predicting the end point potential break values: A case of potentiometric titration of lipophilic anions with cetylpyridinium chloride. *Microchem. J.* **2021**, *160*, 105758. <https://doi.org/10.1016/j.microc.2020.105758>.
10. Fizer, O.; Fizer, M.; Sidey, V. Quantum chemical insight on the uranyl benzoates association with cetylpyridinium. *J. Radioanal. Nucl. Chem.* **2021**, *329*, 661–670. <https://doi.org/10.1007/s10967-021-07843-4>.
11. Samardžić, M.; Budetić, M.; Széchenyi, A.; Marković, D.; Živković, P.; Šarkanj, B.; Jozanović, M. The novel anionic surfactant selective sensors based on newly synthesized quaternary ammonium salts as ionophores. *Sens. Actuators B Chem.* **2021**, *343*, 130103. <https://doi.org/10.1016/j.snb.2021.130103>.
12. Mao, X.; Auer, D.L.; Buchalla, W.; Hiller, K.-A.; Maisch, T.; Hellwig, E.; Al-Ahmad, A.; Cieplik, F. Cetylpyridinium chloride: mechanism of action, antimicrobial efficacy in biofilms, and potential risks of resistance. *Antimicrob. Agents Chemother.* **2020**, *64*, e00576. <https://doi.org/10.1128/AAC.00576-20>.
13. Becker, K.; Brunello, G.; Scotti, L.; Drescher, D.; John, G. Efficacy of 0.05% chlorhexidine and 0.05% cetylpyridinium chloride mouthwash to eliminate living bacteria on in situ collected biofilms: an in vitro study. *Antibiotics* **2021**, *10*, 730. <https://doi.org/10.3390/antibiotics10060730>.
14. Steyer, A.; Marušić, M.; Kolenc, M.; Triglav, T. A Throat lozenge with fixed combination of cetylpyridinium chloride and benzydamine hydrochloride has direct virucidal effect on SARS-CoV-2. *COVID* **2021**, *1*, 435-446. <https://doi.org/10.3390/covid1020037>.
15. Alam, S.S.; Mather, C.B.; Seo, Y.; Lapitskya, Y. Poly(allylamine)/tripolyphosphate coacervates for encapsulation and long-term release of cetylpyridinium chloride. *Colloid Surf. A-Physicochem. Eng. Asp.* **2021**, *629*, 127490. <https://doi.org/10.1016/j.colsurfa.2021.127490>.
16. Teoman, B.; Muneeswaran, Z.P.; Verma, G.; Chen, D.; Brinzari, T.V.; Almeda-Ahmadi, A.; Norambuena, J.; Xu, Sh.; Ma, Sh.; Boyd, J.M.; Armenante, P.M.; Potanin, A.; Pan, L.; Asefa, T.; Dubovoy, V. Cetylpyridinium trichlorostannate: synthesis, antimicrobial properties, and controlled-release properties via electrical resistance tomography. *ACS Omega* **2021**, *6*, 35433–35441. <https://doi.org/10.1021/acsomega.1c04034>.
17. Li, C.; Yao, J.; Zhang, T.C.; Xing, W.; Liang, Y.; Xiang, M. Simultaneous removal of nitrogen and phosphorus by cetylpyridinium bromide modified zeolite. *Water Sci. Technol.* **2017**, *76*, 2895-2906. <https://doi.org/10.2166/wst.2017.459>.
18. Prajitno, M.Y.; Tangparitkul, S.; Zhang, H.; Harbottle, D.; Hunter, T.N. The effect of cationic surfactants on improving natural clinoptilolite for the flotation of cesium. *J. Hazard. Mater.* **2021**, *402*, 123567. <https://doi.org/10.1016/j.jhazmat.2020.123567>.
19. Ren, H.-X.; Zhang, N.; Wu, D.-J.; Neckenig, M.; Jiang, J.-H.; Qi, A.-J.; Li, X.-M.; Ma, Y.-S. Comparative study on adsorption of Cr(VI), Mn(VII), Pb(II) and Cd(II) from aqueous solution using cetylpyridinium bromide-modified zeolite. *Sci. Adv. Mater.* **2019**, *11*, 41-49. <https://doi.org/10.1166/sam.2019.3372>.

20. Ghifari, M.A.; Nuraini, A.; Permatasari, D.; Kamila, N.; Imanullah, T.; Astuti, Y. Nano-zeolite modification using cetylpyridinium bromide for the removal of remazol black B and remazol yellow G dyes. *Adv. Sci. Lett.* **2017**, *23*, 6502-6505. <https://doi.org/10.1166/asl.2017.9667>.
21. Hedayati, M.S.; Li, L.Y. Removal of polycyclic aromatic hydrocarbons from aqueous media using modified clinoptilolite. *J. Environ. Manage.* **2020**, *273*, 111113. <https://doi.org/10.1016/j.jenvman.2020.111113>.
22. Marković, M.; Daković, A.; Rottinghaus, G.E.; Kragović, M.; Petković, A.; Krajišnik, D.; Milić, J.; Mercurio, M.; de Gennaro, B. Adsorption of the mycotoxin zearalenone by clinoptilolite and phillipsite zeolites treated with cetylpyridinium surfactant. *Colloids Surf. B* **2017**, *151*, 324-332. <https://doi.org/10.1016/j.colsurfb.2016.12.033>.
23. Naoe, T.; Hasebe, A.; Horiuchi, R.; Makita, Y.; Okazaki, Y.; Yasuda, K.; Matsuo, K.; Yoshida, Y.; Tsuga, K.; Abe, Y.; Yokoyama, A. Development of tissue conditioner containing cetylpyridinium chloride montmorillonite as new antimicrobial agent: Pilot study on antimicrobial activity and biocompatibility. *J. Prosthodont. Res.* **2020**, *64*, 436-443. <https://doi.org/10.1016/j.jpor.2019.12.002>.
24. Yamamoto, Y.; Yoshihara, K.; Nagaoka, N.; Van Meerbeek, B.; Yoshida, Y. Novel composite cement containing the antimicrobial compound CPC-Montmorillonite. *Dent. Mater.* **2022**, *38*, 33-43. <https://doi.org/10.1016/j.dental.2021.10.009>.
25. Hatakeyama, T.; Liu, Z. Handbook of Thermal Analysis, Wiley, **1998**, <https://www.wiley.com/en-us/Handbook+of+Thermal+Analysis-p-9780471983637>.
26. Boettinger, W.J.; Kattner, U.R.; Moon, K.-W.; Perepezko, J.H. DTA and heat-flux DSC measurements of alloy melting and freezing, in: J.-C. Zhao (Eds.), Methods for Phase Diagram Determination, Elsevier Science Ltd, **2007**, 151-221, <https://doi.org/10.1016/B978-008044629-5/50005-7>.
27. Milyovich, S.S.; Gomonaj, V.I.; Kovalčíková, A.; Shepa, I.; Molčanová, Z.; Barchiy, I.E.; Pavlyuk, V.V.; Stercho I.P. Chemical composition and crystal structure of the natural clinoptilolite deposit of Sakyrnitsya and its modified forms. *Sci. Bull. Uzhh. Univ. Ser. Chem.* **2019**, *42*, 73-80. <https://doi.org/10.24144/2414-0260.2019.2.73-80>.
28. Paradies, H.H.; Habben, F. Structure of N-hexadecylpyridinium chloride monohydrate. *Acta Crystallogr. C* **1993**, *49*, 744-747. <https://doi.org/10.1107/S010827019201179X>.
29. Farjoo, A.; Sawada, J.A.; Kuznicki, S.M. Manipulation of the pore size of clinoptilolite for separation of ethane from ethylene. *Chem. Eng. Sci.* **2015**, *138*, 685-688. <https://doi.org/10.1016/j.ces.2015.08.044>.
30. Rowland, R.S.; Taylor, R. Intermolecular nonbonded contact distances in organic crystal structures: comparison with distances expected from van der Waals radii. *J. Phys. Chem.* **1996**, *100*, 7384-7391. <https://doi.org/10.1021/jp953141>.
31. Becker, K.; Brunello, G.; Scotti, L.; Drescher, D.; John, G. Efficacy of 0.05% chlorhexidine and 0.05% cetylpyridinium chloride mouthwash to eliminate living bacteria on in situ collected biofilms: an in vitro study. *Antibiotics* **2021**, *10*, 730. <https://doi.org/10.3390/antibiotics10060730>.
32. Watanabe, E.; Tanomaru, J.M.G.; Piacuzzi Nascimento, A.; Matoba Junior, F.; Tanomaru Filho, M.; Filho, Ito, I.Y. Determination of the maximum inhibitory dilution of cetylpyridinium chloride-based mouthwashes against *Staphylococcus aureus*: an in vitro study. *J. Appl. Oral. Sci.* **2008**, *16*, 275-279. <https://doi.org/10.1590/S1678-77572008000400009>.
33. Edlind, M.P.; Smith, W.L.; Edlind, T.D. Effects of cetylpyridinium chloride resistance and treatment on fluconazole activity versus *Candida albicans*. *Antimicrob. Agents Chemother.* **2005**, *49*, 843-845. <https://doi.org/10.1128/AAC.49.2.843-845.2005>.